A High Wind Statistical Prediction Model for the Northern Front Range of Colorado

DANIEL T. LINDSEY
NOAA/NESDIS/STAR/RAMMB, Fort Collins, Colorado

Brian McNoldy, Zachary Finch, David Henderson, David Lerach, Robert Seigel, Jesse Steinweg-Woods, Elizabeth Stuckmeyer, Darren Van Cleave, Gabriel Williams, and Molly Woloszyn
Dept. of Atmospheric Science, Colorado State University, Fort Collins, Colorado

(Manuscript received 30 November 2010; in final form 26 April 2011)

ABSTRACT

Numerical models occasionally struggle with forecasting certain meteorological events, so statistical methods can be employed to aid operational forecasters. One example is high wind events along the Front Range of the Rocky Mountains in northern Colorado. During the cool season, fair-weather wind events can produce gusts exceeding 35 m s^{-1}, sometimes resulting in widespread damage. In this study, we build on previous research on Colorado high wind events and describe the development of a statistical model that is now running in real-time. Given the abundance of reanalysis data now available, similar models could be built for a variety of applications in other parts of the country or the world.

1. Introduction

While numerical models have improved dramatically over the last decade, some meteorological phenomena are still either not resolved or are poorly forecast by the models. One example is hurricane intensity. Models have difficulty adequately representing eye wall convective processes, so statistical techniques have been developed to produce intensity forecasts (e.g., SHIPS, DeMaria et al. 2005). Today, these statistical forecasts continue to out-perform the dynamical model intensity forecasts (Franklin 2010). Another example used extensively by the National Weather Service (NWS) is Model Output Statistics (MOS, Kalnay 2003). MOS uses

Corresponding author address: Dr. Daniel T. Lindsey, CIRA/Colorado State University, 1375 Campus Delivery, Ft. Collins, CO 80523-1375
E-mail: Dan.Lindsey@noaa.gov

model forecasts in a multiple linear regression to improve point forecasts of variables such as surface temperature, and does a good job of correcting model biases. Given the wealth of reanalysis data now available, it stands to reason that similar statistical techniques can be applied to other meteorological problems that are not forecasted well by the models, such as high wind events along the Front Range of Colorado.

Downslope windstorms are relatively common in the lee of the Rocky Mountains, particularly in the autumn, winter, and spring. A few previous studies have looked at high wind events along the Colorado Front Range; most have focused on windstorms in Boulder, while a few specifically highlighted Fort Collins (e.g., Cotton et al. 1995). Recently, Mercer et al. (2008) examined a variety of statistical techniques and predictors to study downslope windstorms in Boulder. They used radiosonde observations as the sole data source, so biases between sounding data and numerical model output may limit the utility of applying this method to future forecast times. Weaver and Phillips (1990) looked specifically at Fort Collins windstorms and concluded that the best predictors are sea level pressure gradient, 700 hPa geopotential height gradient, and the existence of a dome of cold air over Fort Collins and the adjacent plains. In the present study, we employ a statistical technique to examine Fort Collins high wind events that have occurred over the twelve year period 1997-2009, and examine possible predictor variables for severe wind events, thus building on the work by Weaver and Phillips (1990). However, the primary purpose of the paper is to illustrate how such a statistical method might be used to assist operational forecasters.

2. Data and High Wind Event Selection

Surface wind data for this study are obtained from the Christman Field Weather Station (40.60 °N, 105.14 °W), located roughly 5.5 km west of downtown Fort Collins in a large open field far from any structures or obstacles (Figs. 1 and 2). Nearly continuous five-minute-average observations of 10 m wind speed and direction are available from September 1997 to the present. (Most surface stations used by the NWS measure surface winds as two-minute averages, so Christman Field will necessarily show lower sustained wind values.) In order to focus on fair weather wind events and avoid convective wind gusts, only data from October to April are considered, as the majority of windstorms occur during these months. For the purpose of this study, we define a high wind event as one in which the five-minute-average wind exceeded 17.9 m s^{-1} (40 mph) *or* a wind gust exceeded 25.9 m s^{-1} (58 mph). Two convective wind gusts were manually removed from the list of high wind events. A wind gust was determined to be "convective" if the sustained 5-minute winds did not exceed 10 m s^{-1} for 10 minutes before and after the gust. The NWS criteria for a high wind event in Fort Collins are stricter than this. In fact, using their criteria, there has been only one event in the last 13 years (the first entry in Table 1). Attempting to create a statistical model to predict such a rare event is not feasible, so we decided to use the less strict criteria, one more similar to the criteria used for the eastern plains of Colorado by the NWS. Each event was matched in time to the nearest corresponding North American Regional Reanalysis (NARR, Mesinger et al. 2006) three-hourly UTC analysis. A few of the chosen events lasted long enough to be covered by multiple NARR times; these were counted as a single event, and the adjoining high wind analyses were omitted from the analysis discussed in Section 4. Thirty-eight total events were identified. Table 1 shows five of the chosen cases, listed in order of the strongest maximum wind gust, and Figure 3 shows the monthly distribution of the events.

3. High Wind Predictors

In virtually every paper discussing Front Range windstorms, events are categorized as either "chinook" or "bora" depending on certain synoptic conditions. Chinook events are often associated with a lee trough and are considered "pre-frontal," meaning they lack strong cold advection at the surface. Bora events occur behind surface cold fronts and are often accompanied by a deepening surface low northeast of Colorado, usually in Nebraska or the Dakotas. We examined the synoptic conditions associated with each of the 38 Christman Field high wind events, and categorized each as chinook or bora. Following Mercer et al. (2008), the 700-500 hPa geostrophic wind direction shear was calculated by taking the difference between the geostrophic wind direction at 500 hPa and the geostrophic wind direction at 700 hPa. Cases that had a difference greater than 15° imply cold advection within that layer, and were classified as bora events. Those with less than 15° wind direction difference were labeled chinook events. Twenty-seven of the 38 cases were classified as bora events and 11 as chinook events.

Figure 4 shows maps of mean MSLP, surface temperatures, 700 hPa heights and 700 hPa wind speeds for the chinook and bora events. Both cases show the center of a surface low located north and east of Colorado with relatively high pressure in western Colorado, resulting in a roughly east-west-oriented MSLP gradient across the mountains of central Colorado. At 700 hPa, both cases show geostrophic winds out of the north of west, with the strongest winds located in southeast Wyoming. The synoptic patterns evident in Fig. 4 are sufficiently similar to one another that the same set of predictors will be used for both types of high wind events (thus requiring no objective distinction between them). Based on Fig. 4 along with previous research of Front Range windstorms (e.g. Mercer et al. 2008, Weaver and Phillips 1990, Lee et al. 1989), variables examined in this study include: mean sea level pressure (MSLP) gradient between Fort Collins and Grand Junction, direction and speed of 700 hPa wind (near the top of the Continental Divide) at grid points roughly west of Fort Collins, whether cold or warm air advection was underway at the surface, whether a stable layer was present (and at what level it was observed), the isobaric gradient of potential temperature in a vertical cross-section to the west of Fort Collins, the location of a 300 hPa jet streak, and whether or not a cold dome of low potential temperature air was present over Fort Collins. NARR data were viewed for each case, and the following potential predictors were excluded: temperature advection - in almost every case, cold advection was observed, but the strength of the advection varied; stable layer – a stable layer was observed in most cases, but its magnitude and vertical placement varied greatly; location of the 300 hPa jet streak - this varied greatly. It should also be noted that the largest surface wind speed at the NARR grid point closest to Christman Field in the entire dataset was less than 16 m s^{-1}, so the NARR has a low bias in surface wind speed for high wind events, as we expected.

Based on the analysis described above, the following were initially selected as predictors: 1) The east/west potential temperature difference along the 650 hPa pressure surface between grid points C and E (see Figs. 5 and 6 for these locations and for clarification), 2) The difference in MSLP between grid points A and E, 3) The magnitude and direction of the 700 hPa wind vector at grid point D, 4) The difference in the 700 hPa height between grid points B and E, 5) The difference in potential temperature between 700 hPa and the surface at grid point E, and 6) The surface temperature at point E. Figure 5 displays an example map of NARR MSLP from 30 Dec 2008 at 0600 UTC. Points A and E were chosen for the MSLP difference calculation because the strongest gradient was typically observed between these areas in the high wind cases. Additionally, the mean surface wind direction at Christman Field during the high wind events was 279°, so the flow had a large isallobaric component. Air descending from the west to east was therefore assumed to originate roughly to the west of Ft. Collins at higher levels. Figure 6 shows an example from the same case as above of an east-west vertical cross section of potential temperature and vertical velocity that passes near Fort Collins. Note the downward motion near 650 hPa and 105.25° W, and the associated downward-sloping isentropes. This signature was present in every case and was the motivation for choosing predictor 1) above.

4. Statistical Analysis and Validation

In order to properly perform a statistical analysis, both the "positive" high wind cases and the "negative" cases (meaning no high winds were observed within a 6-hour period) must be included. Since only the 6-hourly (00, 06, 12, and 18 UTC) NARR files are locally available, only these will be analyzed for the negative cases. The entire dataset consists of 10187 NARR analyses. We first determined thresholds for several of the variables which eliminated as many negative cases as possible while leaving all of the positive cases. Thresholds include a restriction on the speed and direction of the 700 hPa wind at a grid point (D) over the high terrain west of Fort Collins. Almost every case occurred after the passage of a 700 hPa trough axis, so the 700 hPa wind direction is required to be from between 250-330º and its speed more than 10 m s^{-1}. High wind events also occur in the absence of a cold dome at the surface, so the surface temperature is forced to be warmer than 266 K. Filtering the NARR data with the thresholds listed in Table 2 left only 1407 cases, including all of the positive cases.

Wilks (2006) states that logistic regression is specifically designed for creating a statistical model that outputs probability forecasts. Such forecasts have the advantage of inherently including uncertainty information, as opposed to a binary forecast of 'yes' or 'no'. From Wilks (2006), logistic regressions (with 5 predictors) are fit to yes/no predictands according to the nonlinear equation

$$p = \frac{1}{1 + \exp(-b_0 - b_1 x_1 - b_2 x_2 - b_3 x_3 - b_4 x_4 - b_5 x_5)}, \tag{1}$$

where p is the predicted probability, x_n are the predictors, and b_n are the coefficients that determine the best fit. Fortran code to perform logistic regression was obtained courtesy of Alan Miller at http://jblevins.org/mirror/amiller/. One of the outputs from this code is the log-likelihood, or the logarithm of the likelihood function. According to Wilks (2006), a likelihood ratio test (using their Eq. 5.19) may be used to see whether adding a predictor provides a statistically significant improvement to the model compared to a model without the predictor. In order to make sure all five of our potential predictors should be used, we built a model using all combinations of the five predictors; this includes cases using a single predictor, two, three, four and all five, so there are 31 total possibilities. For each one, the likelihood ratio test was used to compare it to the case using all 5 predictors, and the resulting chi-squared value was used to determine significance level. After this analysis, it was determined that the 5-predictor model was not significant to the 95% level compared to the model using only four predictors excluding the 700 hPa height difference. We therefore concluded that this predictor should not included in the model, so the new probability function becomes

$$p = \frac{1}{1 + \exp(-b_0 - b_1 x_1 - b_2 x_2 - b_3 x_3 - b_4 x_4)}. \tag{2}$$

Table 3 lists the resulting coefficients after performing the regression using all 1407 of the post-thresholded 6-hourly cases. The normalized coefficients are provided to see which of the predictors get relatively more weight, and the raw coefficients are the ones used in Eq. (2) and are multiplied by the predictors having the proper MKS units. For completeness, the constant b_0 has a raw value of -9.84 and -8.83 for the full and subsetted dataset, respectively.

In order to validate this model, the logistic regression was rerun after excluding the final 2 high wind seasons (1997-1998 and 1998-1999), or 20% of the data. Table 3 also lists (on row 3) the raw coefficients after using this data subset. The differences in the coefficients of the predictors are relatively small. Next, probabilities were calculated for the independent dataset that was excluded from the analysis above using Eq. (2) and the subset coefficients. Fig. 7 is a histogram summarizing the results. Before calculating the probabilities, the thresholds from Table 2 were applied to the data, and 1358 of the 6-hour periods were automatically assigned a 0% probability; these are not represented in Fig. 7. Note that the largest forecast probability (66%) was an observed 'yes' event. One of the five forecasts between 20-40% had high winds, one of the 16 in the 10-20% range were yeses, as was one of the 23 forecasts in the 5-10% range. By design, the bias of the dependent dataset is zero. To calculate the bias in the independent dataset, we simply add up all forecast probabilities to get 931%. Since there were only 5 observed high wind events in this time period, a zero bias would mean the probability sum should be 500%, meaning there is a high bias by almost a factor of two.

Another means to validate the model on the independent dataset is using the Brier Skill Score (BSS). As explained in Wilks (2006) and employed by Schumacher et al. (2009), the Brier Score (BS) is the mean squared error of the probability forecasts, or

$$BS = \frac{1}{n}\sum_{k=1}^{n}(y_k - o_k)^2 \ , \qquad (3)$$

and BSS is defined as

$$BSS = 1 - \frac{BS}{BS_{ref}}, \tag{4}$$

where n is the number of forecast-event pairs, y_k are the forecast probabilities, and o_k are the observed probabilities. BS_{ref} is a reference score for which we'll use the climatological probability from the dependent dataset, or 38/8480 (0.389%). The BS turns out to be 0.00205, compared to a BS_{ref} of 0.00294, resulting in a BSS of 0.301, or a ~30% improvement over a climatological forecast.

An alternate validation procedure involves choosing a threshold probability such that all forecasts above that value are considered 'yes' forecasts and all below that value are considered 'no' forecasts. The advantage of this method is the ability to calculate familiar statistics such as the Probability of Detection (POD). The threshold providing the most favorable validation results of the independent dataset turns out to be 22%. Using this, there were three predicted yeses that had observed wind events, four predicted yeses in which no high wind event was observed, and two predicted no's in which high wind events were observed. Using the equations from Wilks (2006), this results in a POD of 0.60, a False Alarm Ratio of 0.57, a Critical Success Index (CSI) of 0.33, and a Bias of 1.40. The relatively high number of false alarms causes the CSI to be lower than desired. These results underscore the difficulty in predicting an event based on a hard wind speed threshold; often, an observed event barely crosses the threshold, and other times a non-event almost reaches the threshold.

5. Real-Time Model

A real-time version of this high wind prediction model has been implemented to assist local forecasters. Since NARR data generally become available at least one month after real-time, a different data source is needed to make high wind probability forecasts. The North American Mesoscale (NAM) model was chosen; it has 40-km grid spacing, provides 3-hour forecasts out to 84 hours, and a new run is performed every 6 hours. Although the 32-km NARR data has a similar resolution to the 40-km NAM, biases might exist between them, resulting in degraded forecasts. This is a problem with no easy solution, as the NAM is not available back to 1997.

Every six hours, the NAM output is obtained and the probability model is applied to both the analysis time and every 6 hours out to 84 hours, thus providing a probability of high winds out to 3.5 days in the future. Output is currently displayed on this page: http://einstein.atmos.colostate.edu/~mcnoldy/highwind/. Figure 8 shows an example of how the model output appears on this webpage. The dark blue line shows the past analyses, and the light blue line shows the current analysis and forecast out to 84 hours. For this particular forecast, the model shows a ~13% probability of high winds for the 24-hour forecast and a ~50% probability at 78 hours. Real-time NAM data will be collected over the next several seasons so that any biases between the the NARR and NAM can be corrected.

6. Summary

A statistical model to forecast high wind probability in Fort Collins, CO, was developed and tested. The model uses NAM analyses and forecasts to provide statistical probabilities out to 3.5 days in the future. Model validation using an independent dataset revealed a high bias in the probabilities, but a significant improvement was found over a climatological forecast or a forecast using model forecast surface wind speeds.

Some meteorological problems are not forecast well by numerical models, so using statistical models based on NWP output is sometimes a good solution to improve operational forecasts. The goal of this paper was to present an example of how such a statistical model was developed and how it can be used to assist forecasters. Other problems that might be suitable for statistical forecasting include snow amount forecasts in complex terrain, turbulence forecasts, and high winds in other regions. Future work with high wind forecasting includes using observed geostationary satellite data as a possible predictor, since certain persistent satellite signatures have been qualitatively observed to occur before and during high wind events.

Acknowledgements. This material is based on work supported by the National Oceanic and Atmospheric Administration under Grant NA090AR4320074. The authors would like to thank Mark DeMaria for a very insightful review of this manuscript and John Knaff for assistance with the statistical analysis, in addition to two anonymous reviews who provided excellent suggestions for significant improvements. The views, opinions, and findings in this report are those of the authors, and should not be construed as an official NOAA and/or U.S. Government position, policy, or decision.

REFERENCES

Cotton, W. R., J. F. Weaver, and B. A. Beitler, 1995: An unusual summertime downslope wind event in Fort Collins, Colorado on 3 July 1993. *Wea. Forecasting*, **10**, 786-797.

DeMaria, M., M. Mainelli, L. K. Shay, J. A. Knaff, and J. Kaplan, 2005: Further improvements in the Statistical Hurricane Intensity Prediction Scheme (SHIPS). *Wea. Forecasting*, **20**, 531-543..

Franklin, J. L., 2010: 2009 National Hurricane Center Forecast Verification Report. *http://www.nhc.noaa.gov/verification/pdfs/Verification_2009.pdf*, 71 pp.

Kalnay, E., 2003: *Atmospheric Modeling, Data Assimilation and Predictability*. Cambridge University Press, 341 pp.

Lee, T. J., R. A. Pielke, R. C. Kessler, and J. F. Weaver, 1989: Influence of cold pools downstream of mountain barriers on downslope winds and flushing. *Mon. Wea. Rev.*, **117**, 2041-2058.

Mercer, A. E., M. B. Richman, H. B. Bluestein, and J. M. Brown, 2008: Statistical modeling of downslope windstorms in Boulder, Colorado. *Wea. Forecasting*, **23**, 1176-1194.

Mesinger, F., G. DiMego, E. Kalnay, K. Mitchell, P. C. Shafran, W. Ebisuzaki, D. Jovic, J. Woolen, E. Rogers, E. H. Berbery, M. B. Ek, Y. Fan, R. GruhPaine, W. Higgins, H. Li, Y. Lin, G. Manikin, D. Parrish, and W. Shi, 2006: North American regional reanalysis. *Bull. Amer. Meteor. Soc.*, **87**, 343-360.

Schumacher, A. B., M. DeMaria, and J. A. Knaff, 2009: Objective estimation of the 24-h probability of tropical cyclone formation. *Wea. Forecasting*, **24**, 456-471.

Weaver, J. F., and R. S. Phillips, 1990: An expert system application for forecasting severe downslope winds at Fort Collins, Colorado, U.S.A. Preprints, *16th Conf. Severe Local Storms*, Kananaskis Park, AB, Canada, Amer. Meteor. Soc., 13-15.

Wilks, D. S., 2006: *Statistical Methods in the Atmospheric Sciences*. 2nd ed. Academic Press, 627 pp.

TABLES AND FIGURES

Table 1. Five of the Fort Collins wind events chosen for this study, listed in order of the highest maximum wind gust.

Date	Duration	Maximum Sustained Wind (m s^{-1})	Maximum Wind Gust (m s^{-1})
30 Dec 2008	6 hours	22.3	37.4
8 Apr 1999	4 hours	23.4	32.4
3 Jan 2006	2 hours	19.8	29.9
16 Feb 2007	2 hours	21.6	29.3
13 Nov 2008	1 hour	17.5	29.2

Table 2. Variables and thresholds used to filter the data.

650 hPa theta diff between C and E	MSLP diff between A and E	700 hPa wind speed at D	700 hPa wind direction at D	700 hPa height diff between B and E	theta diff between surface and 700 hPa	Surface temperature at E
> 0.75 K	> 5.0 hPa	> 10.0 m s^{-1}	> 250° and < 330°	> 32.0 gpm	<=14 K	> 266.0 K

Table 3. Variables used in the linear regressions, and the resulting normalized and raw coefficients for the full dataset, and the raw coefficients for the subset of the data.

	650 hPa theta diff between C and E (b_1)	**MSLP diff between A and E (b_2)**	**700 hPa wind speed at D (b_3)**	**theta diff between surface and 700 hPa (b_4)**
Normalized coefficient	0.391	0.839	0.900	-1.328
Raw coefficient	0.368	0.299	0.283	-0.396
Raw coefficient, data subset	0.348	0.283	0.246	-0.389

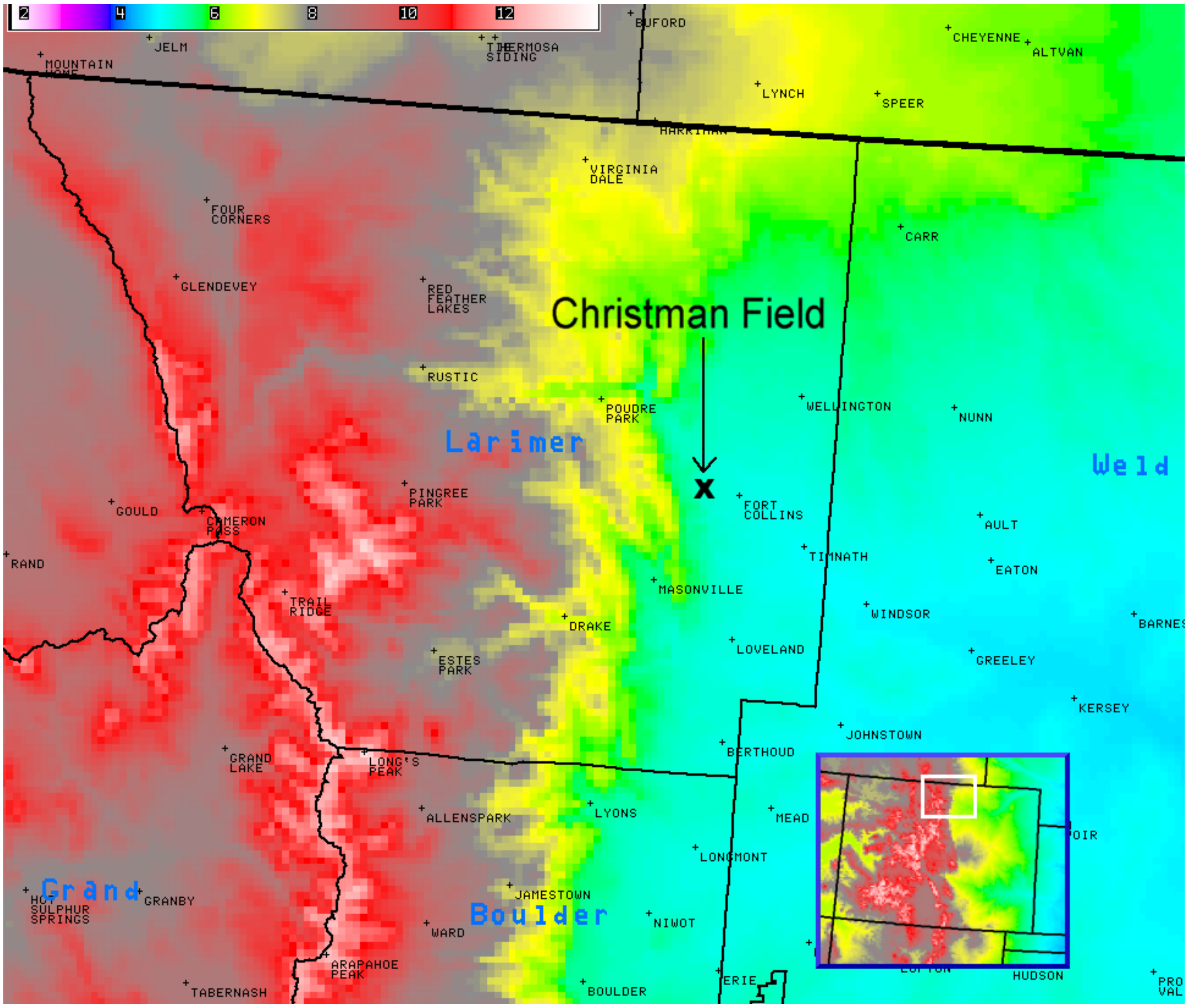

Figure 1. Topographic map of Larimer County, Colorado, with the location of Christman Field denoted with a large 'X'. The inset shows its location within the state of Colorado, and the legend has units of kft.

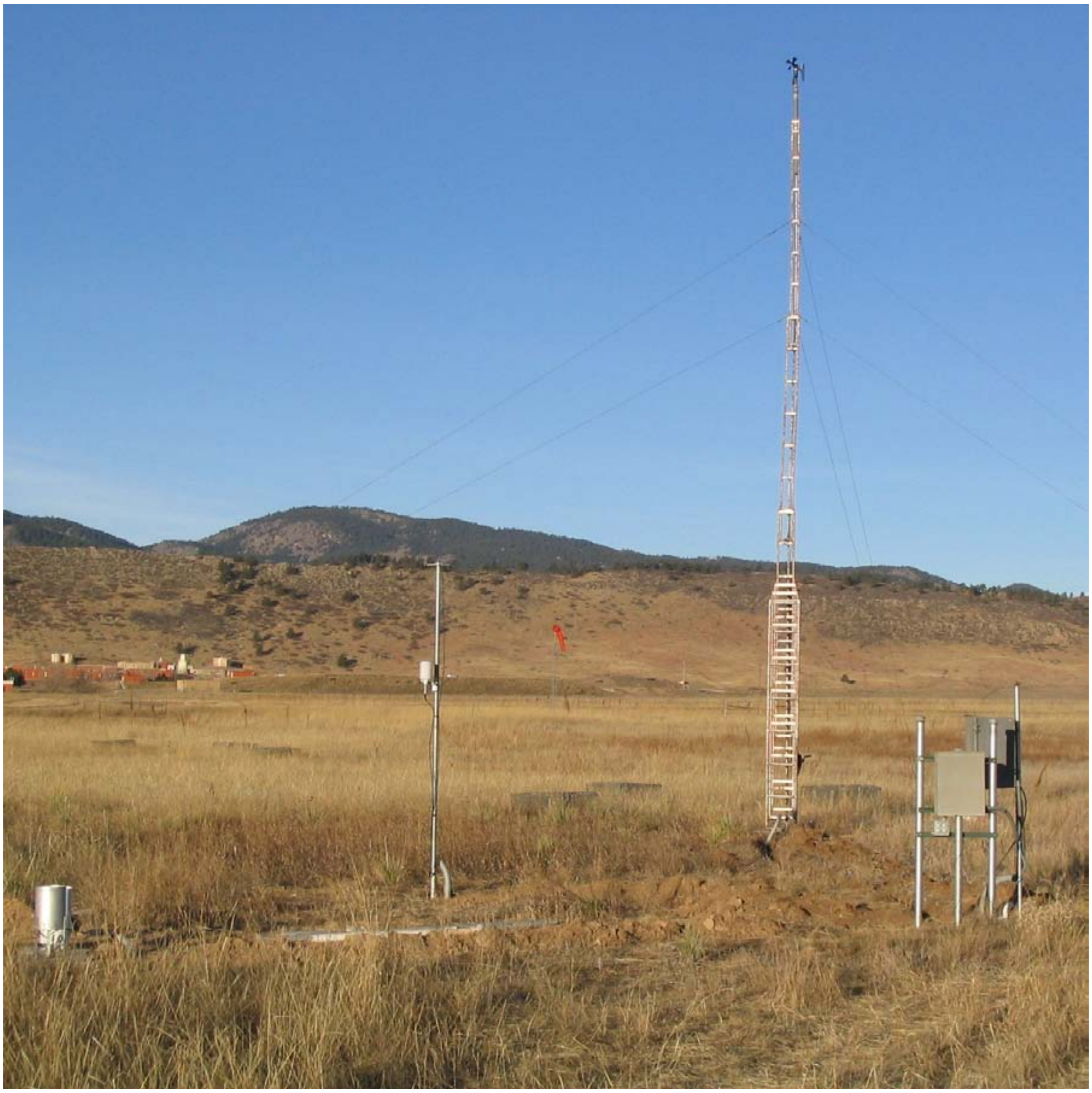

Figure 2. Photo of the Christman Field Weather Station in Fort Collins, CO.

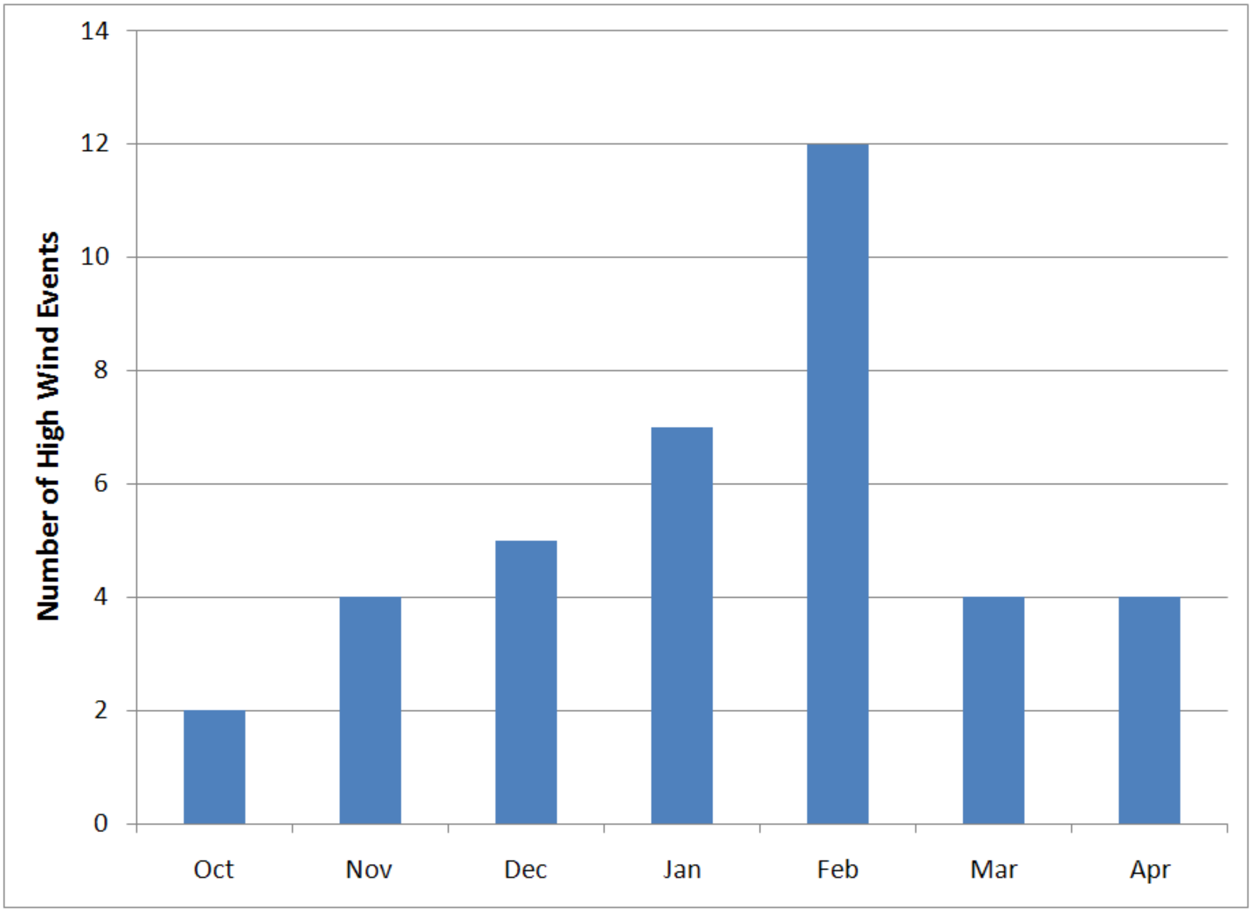

Figure 3. Histogram showing the number of high wind events per month at Christman Field in the developmental dataset from 1997-2009.

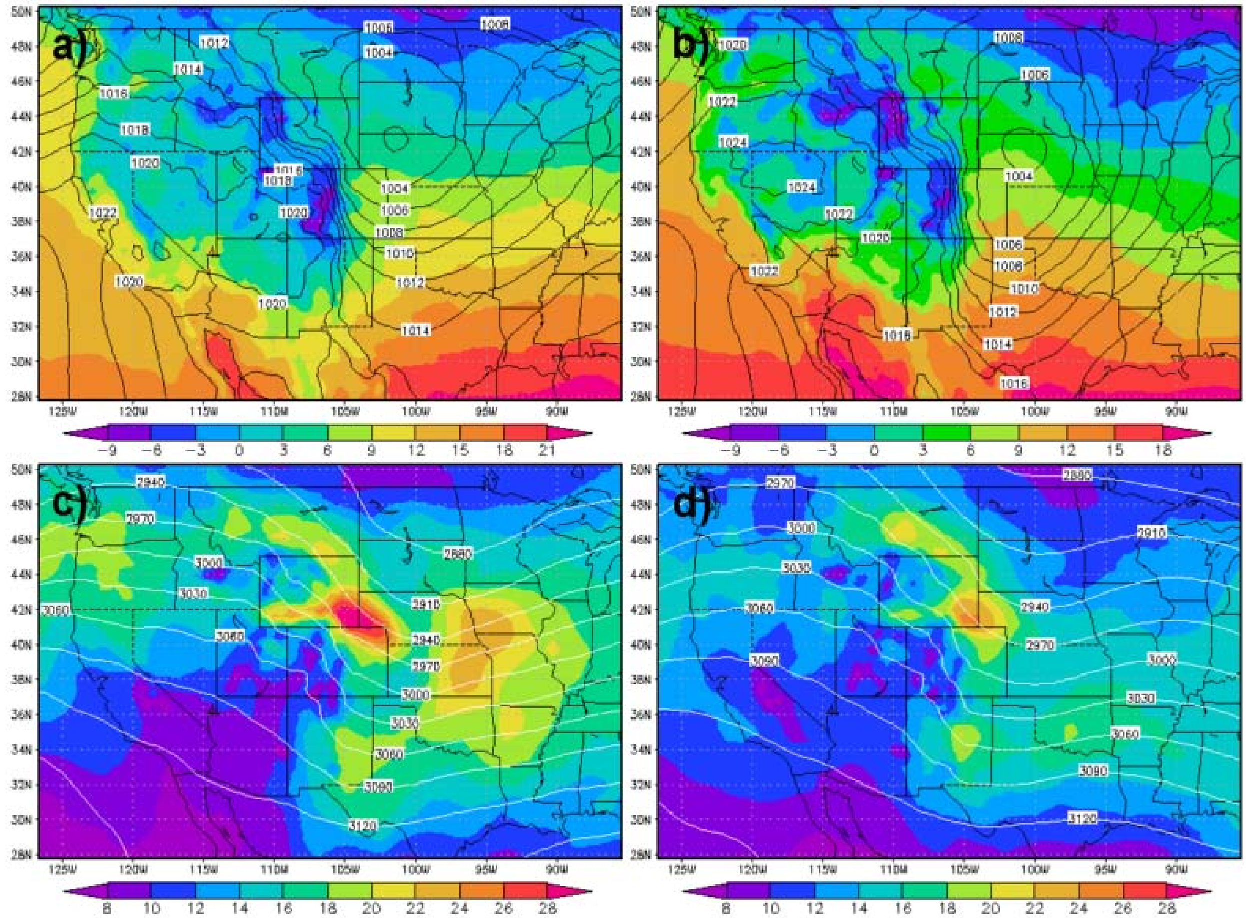

Figure 4. Mean values of the 11 chinook events (a and c) and 27 bora events (b and d), of (a and b) MSLP (contours, hPa) and surface temperature (colors, °C), and (c and d) 700 hPa heights (contours, m) and wind speed (colors, ms^{-1}), from the NARR data.

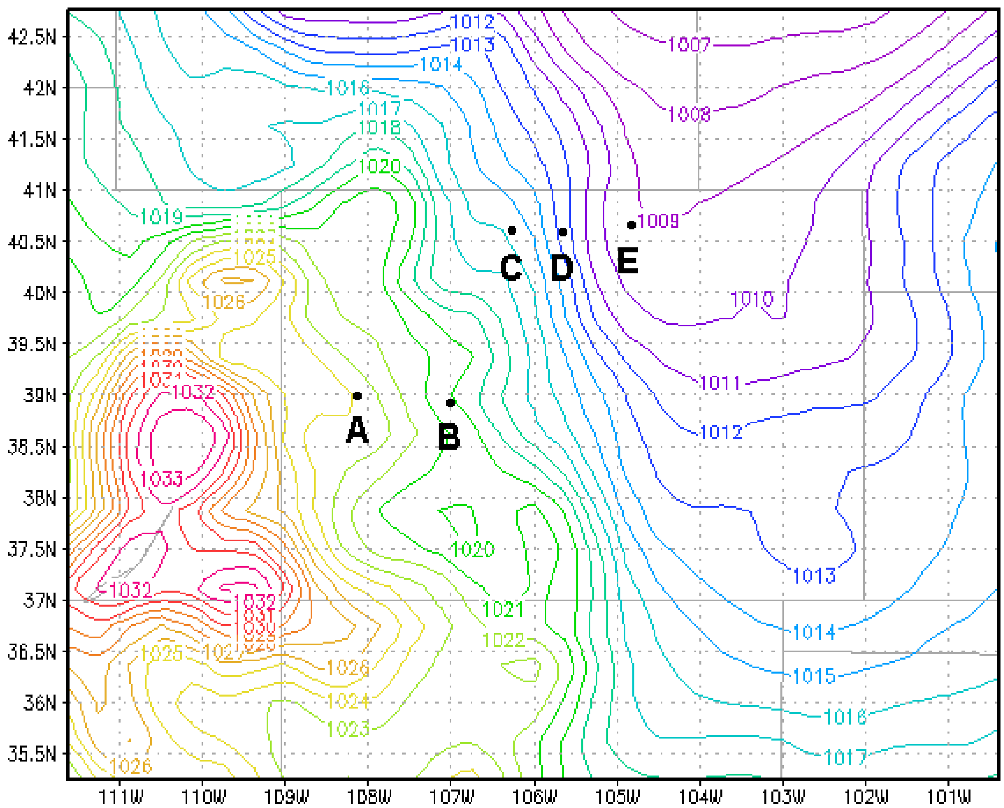

Figure 5. MSLP from the NARR valid at 0600 UTC on 30 December 2008. The points A-E show the locations of the NARR grid points used in the analysis. Christman Field in Fort Collins is located very near grid point E.

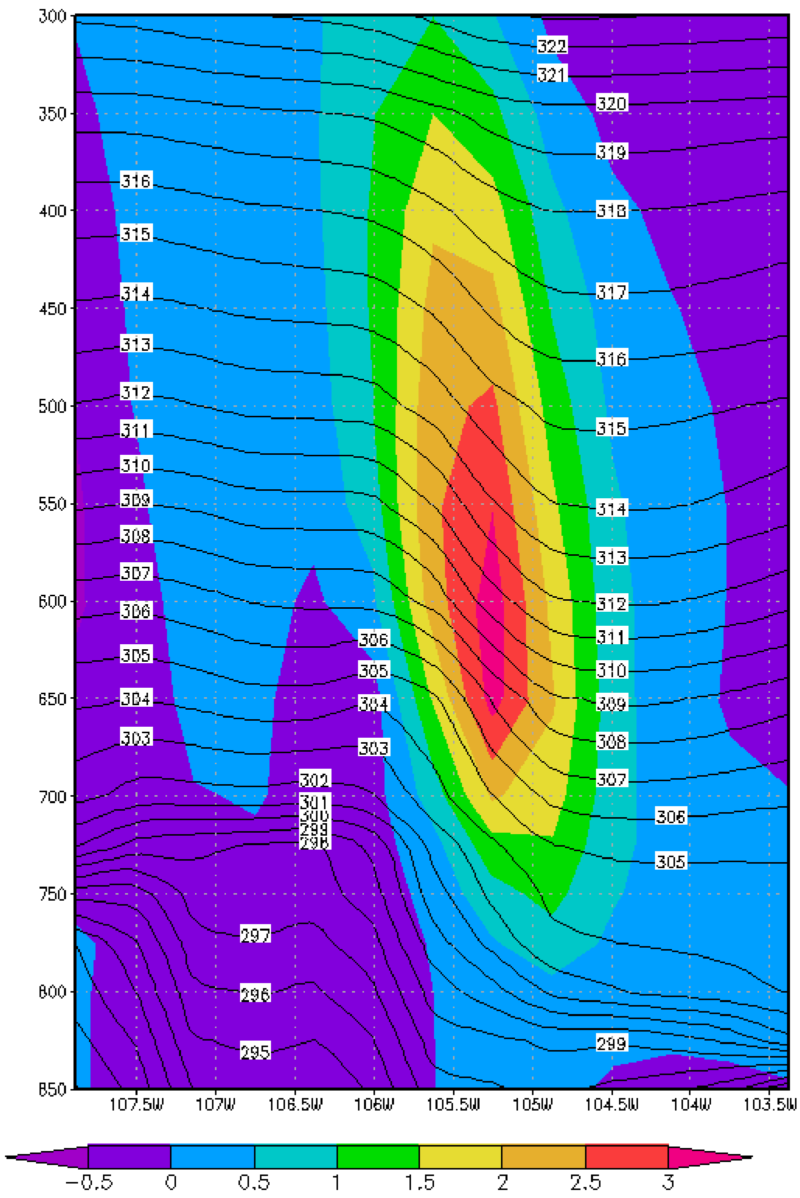

Figure 6. East-west vertical cross-section of potential temperature (contours, K) and pressure vertical velocity (colors, in Pa s^{-1}; positive indicates downward motion) near 40.5° N, from 108°W to near 103.5°W (see Fig. 5 for these longitude locations), from NARR data valid at 0600 UTC on 30 December 2008. Longitude is on the horizontal axis, and pressure in hPa is on the vertical axis.

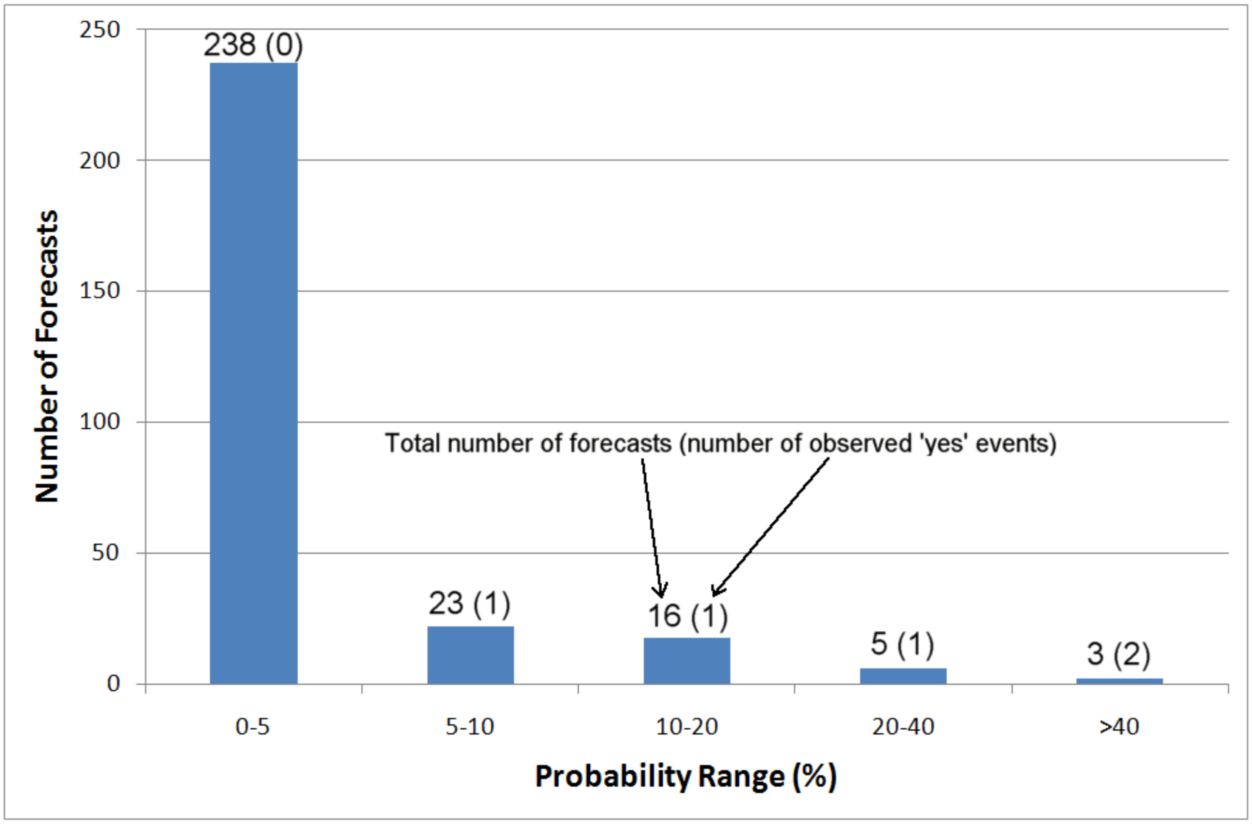

Figure 7. Histogram showing the results of the validation on the independent dataset. The blue bars represent the number of forecast probabilities within several ranges in %, and the number in parentheses are the number of observed 'yes' events that correspond with those forecasts. It should be noted that initial thresholding excluded 1358 6-hour time periods, so those are considered 0% probability forecasts and are not represented on this histogram.

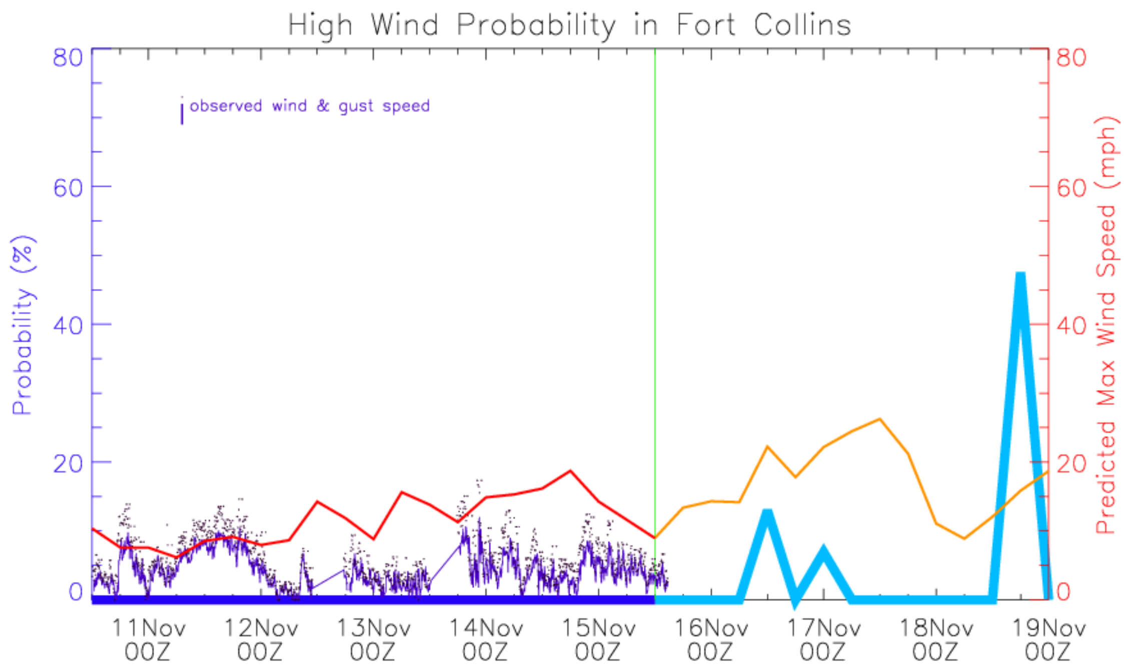

Figure 8. An example of a real-time high wind forecast from 15 November 2010 at 12 UTC. The vertical green line represents the current time (i.e., 12 UTC on 15 November). The dark blue line (to the left of the green line) represents past high wind probability (from the NAM analyses), in this case all 0%. The purple spiky line with dots shows the observed 5-minute sustained winds and gusts from Christman Field. To the right of the vertical green line, the current analysis and forecast for high wind probability is shown by the thick light blue line. The red and orange lines show a predicted maximum sustained wind speed using a different experimental model, and will not be discussed in this paper. A real-time version of this figure can be found here: http://einstein.atmos.colostate.edu/~mcnoldy/highwind/.